TAO, Vol.6, No.2, 197-207, June 1995

Study on the Free Surface Coupling Effect of Seismic Waves

CHIOU-FEN SHIEH[1]

(Manuscript received 24 September 1994, in final form 8 December 1994)

ABSTRACT

This article presents a simple method to calculate the angle of incidence and the slowness of P- and SV-waves from single 3-component set of data. The obtained slowness is used as the parameter to remove the free surface effect, such as phase distortion and amplification, and to recover the original incident wave. This method is derived from the calculation of ratios regarding the horizontal/vertical and the vertical/horizontal response for P-waves and SV-waves, respectively. From the comparison of the calculated ratios with the observed ones (estimated from data), the angle of incidence can be found. Synthetic data are first tested to prove their accuracy, and then, the first P- and SV arrivals of real data are analyzed. The results are compared with those evaluated from polarization analysis, and they appear to be quite consistent for synthetic P-waves.

(Key words: Free surface, Coupling effect, Slowness, Incidence angle)

1. INTRODUCTION

The slowness (or angle of incidence) is the major parameter used to both remove the free surface effect (Jepsen and Kennett, 1990; Kennett, 1991) and to study rupture propagation in the source region (Goldstein and Archuleta, 1991a, b). Jepsen and Kennett (1990) estimate the slowness from array data to remove the free surface effect, and then, decompose observed data into new wavefields. Goldstein and Archuleta (1991b) use frequency-wavenumber techniques with dense array (SMART 1) to obtain more detailed measurements of rupture propagation in the Taiwan area. Dankbaar (1985), using a group of geophones, calculates the slowness and designs P/S filters. In his analyses, an estimated slowness is used for all incident waves. Kennett (1991) roughly estimates the range of the slowness for different wavetypes and isolates them according to the given slowness. In fact however, it is more likely that different body waves reveal with a different degree of slowness. In addition, the slowness is estimated from array data in his analysis (Dankbaar, 1985). For the small array cases, the estimation could be erroneous, thereby making large array data necessary. However, array data are not always available. Hence, this limits the application of his method.

[1] Institute of Seismology, National Chung Cheng University, Taiwan, R.O.C

The purpose of this study is to develop a method which can be applied to every single station to estimate the angle of incidence and the slowness. Moreover, the method must be able to be used for different incident waves independently.

Derived from calculating the ratio of horizontal/vertical and vertical/horizontal for all possible angles of incidence, the method developed is effective for finding the the best fitting to observed ratio computed from peak spectra. It can be called the PEAK SPECTRA METHOD (PSM). In this study, the PSM is first applied to synthetic data to calculate the angle of incidence. The results are then compared with those obtained from polarization analysis. Second, the PSM is applied to the first P- and SV-arrivals (other body waves are also applicable) in real strong motion data. Finally, the recovered incident waves with free surface effect removed are also displayed.

2. THEORY AND METHOD

If only single station 3-component data are available, yet there is some knowledge of the velocity structure regarding P- and S-waves in the neighbourhood of the receiver, the slowness or the angles of incidence of some particular body waves can be determined. From the parameters of the velocity and slowness, the free surface response may be calculated and incident wave may be recovered by removing this response. Kennett's method (1983, 1991) is suitable for calculating near receiver response because the receiver is located at any depth. In the case of a receiver installed on free surface, it is better to use the equations expressed by Dankbaar (1985) or Aki and Richards (1980, Chapter 5). In this paper, the author adopts Dankbaar's (1985) expressions to show the near-receiver response in the slowness-frequency $(p-f)$ domain. For the reader's convenience, Dankbaar's expressions are repeated:

$$R_v^p(p) = \frac{2\zeta(2V_s^2p^2-1)}{\chi R_o(p)}, \tag{1}$$

$$R_v^s(p) = \frac{4V_sp\zeta\eta}{R_o(p)}, \tag{2}$$

$$R_H^p(p) = \frac{4V_pp\zeta\eta}{R_o(p)}, \tag{3}$$

$$R_H^s(p) = \frac{2\eta(1-2V_s^2p^2)}{R_o(p)}, \tag{4}$$

where $\chi = V_s/V_p, \zeta = (\chi^2 - V_s^2p^2)^{\frac{1}{2}}, \eta = (1-V_s^2p^2)^{\frac{1}{2}}$, and $R_o(p) = (1-2V_s^2p^2)^2 + 4p^2V_s^2\zeta\eta$, R with the subscript v or H, and the superscript p or s, respectively represents the response for the vertical or horizontal components for the P- or S-waves.

In this study, only P- and S-arrivals are considered so the vertical and the horizontal component records (U_v and U_H) can be expressed separately for incident P-waves as:

$$U_v(p,f) = P_{in}(p,f)R_v^p(p,f), \tag{5}$$

$$U_H(p,f) = P_{in}(p,f)R_H^p(p,f), \tag{6}$$

and for the incident S-waves as:

$$U_v(p,f) = S_{in}(p,f)R_v^s(p,f), \tag{7}$$

$$U_H(p,f) = S_{in}R_H^s(p,f), \tag{8}$$

where P_{in} and S_{in} represent incident P- and S-waves respectively.

The inverse solution to recover $P_{in}(p,f)$ and $S_{in}(p,f)$ can be expressed as:

$$P_{in}(p,f) = F_v^p(p,f)U_v(p,f) + F_H^p(p,f)U_H^p(p,f), \tag{9}$$

$$S_{in}(p,f) = F_v^s(p,f)U_v(p,f) + F_H^s(p,f)U_H^s(p,f) \tag{10}$$

where

$$F_v^p(p) = \frac{-\chi(1-2V_s^2p^2)}{2\zeta} \tag{11}$$

$$F_H^p(p) = \chi^2 V_p p \tag{12}$$

$$F_v^s(p) = V_s p \tag{13}$$

$$F_H^s(p) = \frac{(1-2V_s^2p^2)}{2\eta} \tag{14}$$

Equations (5) through (8) are modified from Dankbaar's (6) and (7).

With all of the above expressions, the velocities of the P- and S- waves at the free surface and the slowness must be used. The velocities can be obtained from other geophysical methods with the only unknown information remaining, therefore, is the slowness (p). If pure P- or SV-waves, such as the first P or SV arrivals are selected, they can be considered plane waves with the particular slowness approximated. Hence, dividing (6) by (5), the ratio of horizontal/ vertical response for an incident P-wave is:

$$\gamma_p = \frac{U_H(p,f)}{U_v(p,f)} = \frac{R_H^p(p,f)}{R_v^p(p,f)} \tag{15}$$

This ratio is computed in the frequency domain for the windowed signals of P or SV where the horizontal and vertical component time series are both taken to the frequency domain.

Equation (15) is expressed for the entire frequency range with particular slowness. Although the P-wave amplitude spectrum is limited to frequency bands, the background noise covers a wide frequency range. The estimation may well be disturbed by existing noise meaning that the average ratio may be computed from a frequency window whose range covers the peak amplitude spectrum of the vertical component (it is rarely in the peak of the horizontal component). The reason that this is done is that most P-wave energy is recorded

in the vertical component and concentrated in the vicinity of the peak where S/N is high. The computed average ratio $(U_H(p,f)/U_v(p,f))$ is fixed for plane waves. Now, the problem is to find a slowness (or angle of incidence) that can fit the observed ratio. The method is to search a ratio calculated from the right hand side of Equation (15) to fit the observed ratio. Equations (1) and (2) can simply be calculated through 0 to 90 degree, then be substituted into (15) to obtain many calculated ratios, and then compared to the observed ratio to find the best fitting for the angle. The best fitting angle, say θ_p, is the true angle of incidence, and the slowness is calculated from

$$p_i = \frac{sin\theta_p}{V_p}. \tag{16}$$

To remove the free surface effect and to recover the original P- wave, p_i is substituted into Equations (11), (12) and (9).

By letting V_p=0.6, V_s=0.14 km/s for the surface layer, the PSM can be tested with modelling records. The synthetic P-wave incident at different angles is depicted in Figure 1. In this figure, the left side is an incident Ricker wavelet with the central frequency of 30 Hz, while the middle part is the surface record of the vertical (Z) and the horizontal (R) components with the angle of incidence marked in the beginning on the left side. Also, the right side is the recovered P-wave for each corresponding angle of incidence. Theoretically, after the PSM is applied, every recovered P-wave on the right side should be equal to the original Ricker wavelet on the left side, and this is illustrated in the figures. The free surface effect causes different amplification in different components for both P- and SV-waves, but there is no phase shift for the P-wave so the particle motion remains the P type. However, beyond the critical angle $(sin\theta = \frac{V_s}{V_p})$, phase shift happens to the SV-wave, and it becomes a nondispersed surface wave (Ben-Menahan and Sign, 1981). Figure 2 displays the results of the incident SV- wave at different angles of incidence under the same conditions as those in Figure 1. In Figure 2, a phase shift happens to those angles of incidence of a greater degree than that of the critical angle, $13.49°(sin^{-1}(\frac{0.14}{0.6}))$, thereby making the surface records nondispersed surface waves. To recover the incident SV-wave from the surface records, the ratio of vertical/horizontal is estimated by dividing Equation (7) by Equation (8):

$$\gamma_s = \frac{U_v(p,f)}{U_H(p,f)} = \frac{R_v^s(p,f)}{R_H^s(p,f)}. \tag{17}$$

The same procedure as for the P-wave is followed, but Equations (2) and (4) are calculated and substituted into Equation (17) to obtain the angles of incidence and the corresponding slowness. This is substituted Equation (13), (14) and (10), and the original incident SV-wave is recovered and shown on the right side of Figure 2. It is found that the recovered SV-wave are identical to the original ones. From the above two examples, it is proved that

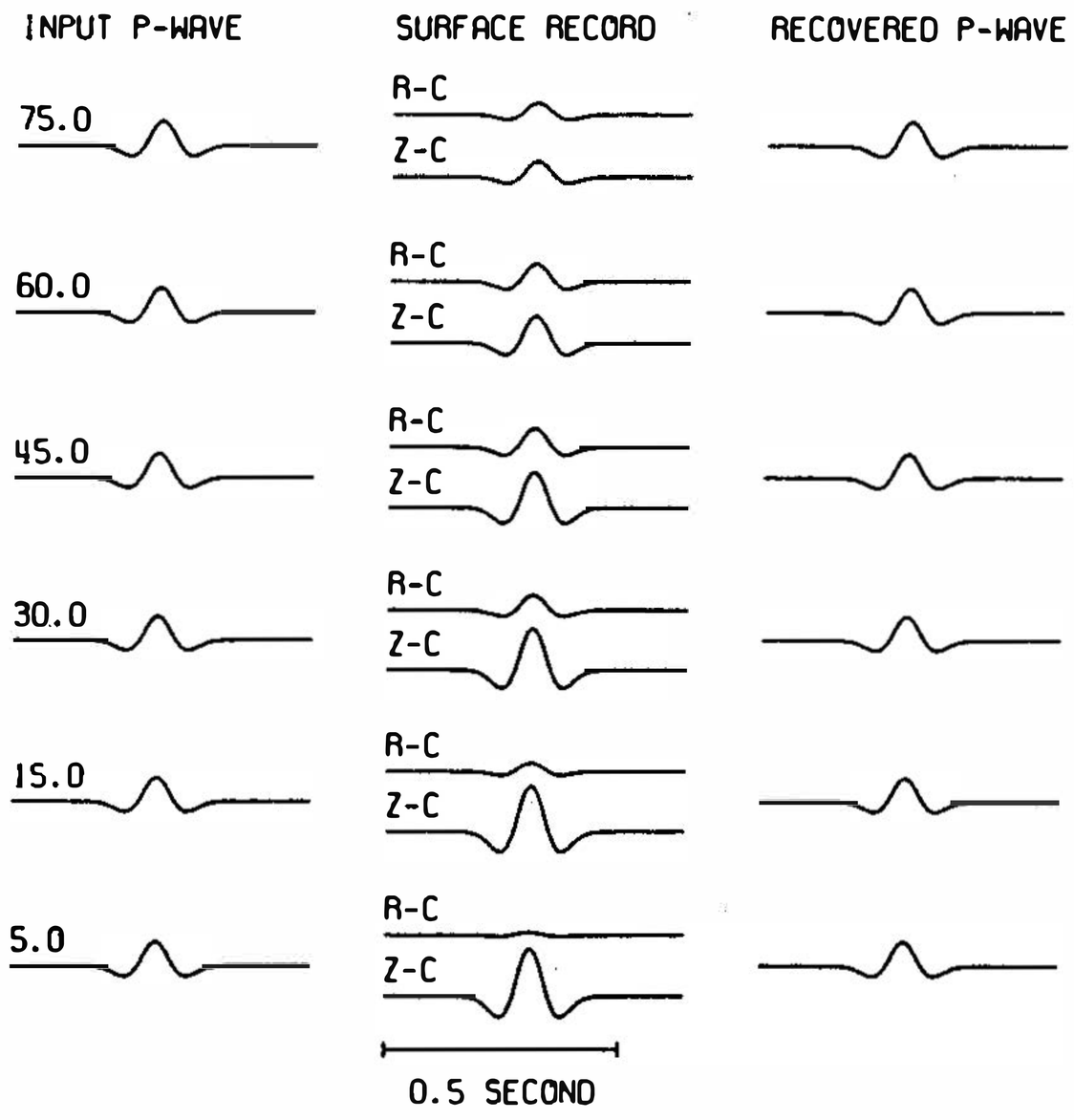

Fig. 1. **The synthetic P type Ricker wavelets with central frequency, 30 Hz, incident in different angles of incidence (marked with a number at the beginning) are depicted on the left. The surface two-component records are shown in the middle. After the PSM is applied to the surface records, the original incident P-waves are recovered as shown on the right.**

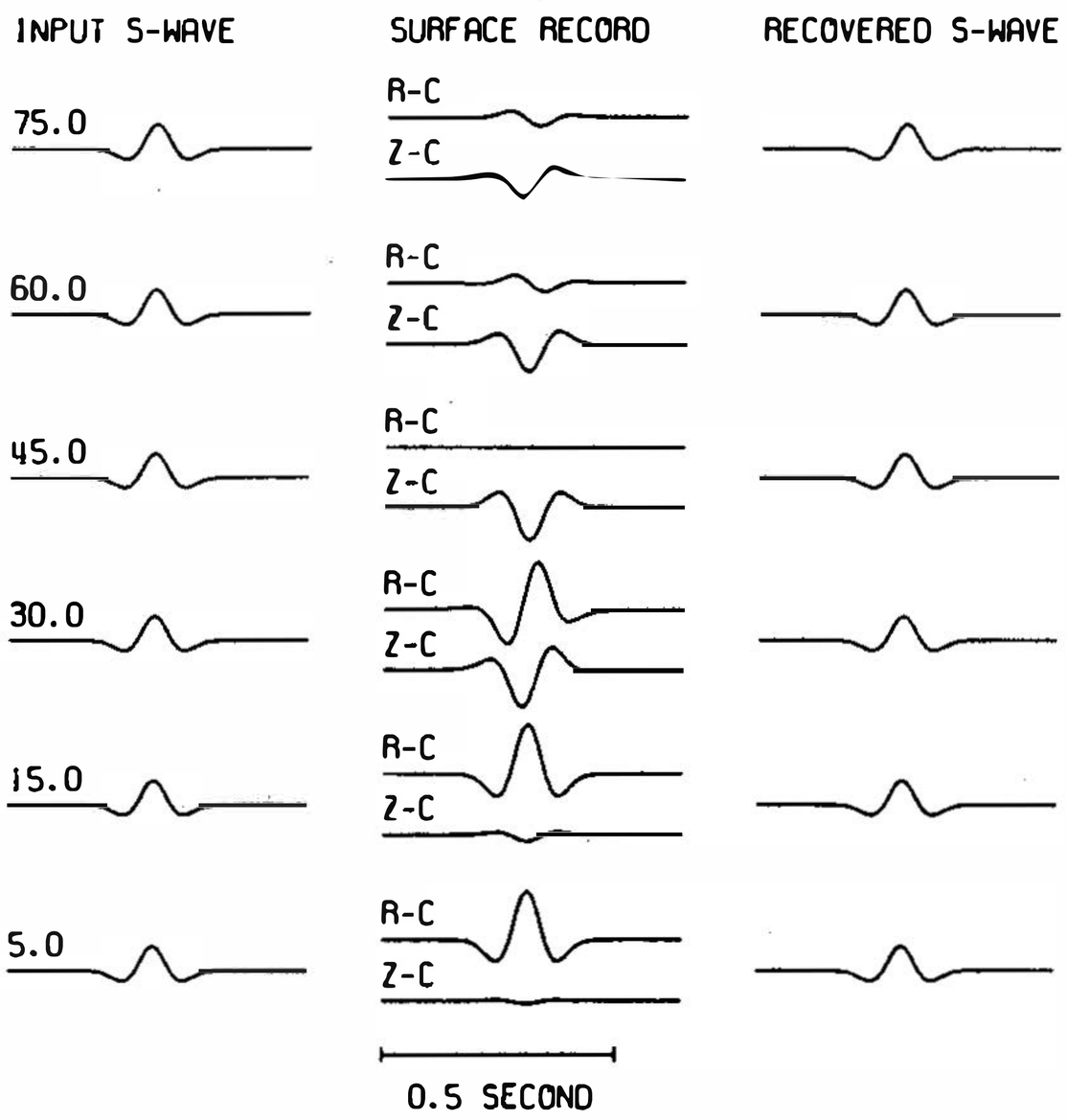

Fig. 2. **The synthetic SV type Ricker wavelets incident in different angles of incidence are depicted on the left. The surface two-component records are shown in the middle. Note that the surface records have become nondisperse surface waves beyond the critical angle (13.49°) due to the free surface effect. After the PSM is applied to the surface records, the original incident SV waves are recovered as shown on the right.**

the PSM plays a useful role in calculating the angle of incidence and the slowness as well as in removing the free surface effect.

A simple polarization analysis (Flinn, 1965) may be adopted to obtain the apparent angle of incidence, ϕ, and then it may be corrected according to:

$$\theta_i = sin^{-1}(sin\frac{\phi}{2}\frac{V_p}{V_s}). \tag{18}$$

However, this modification can only be used for incident P-waves; there is no simple modification for incident SV-wave. To explain this in detail, the examples in Figures 1 and 2 are taken for illustration. With the polarization method (Flinn, 1965), the apparent angle (marked with symbol * in Figure 3) is obtained; after being modified with Equation (18), the results (marked with symbol $\times$ in Figure 3a) are the same as those with the PSM under the noise-free situation. Unfortunately, for the SV-wave, the same result can not be obtained. Besides, SV-waves become nondispersed surface waves beyond a critical angle. Thus, after being processed by the polarization method, only two kinds of apparent angles, 0 and 90 degrees, showed up (Figure 3b). To obtain the real angle of incidence, therefore, the PSM must be employed. Moreover, the polarization method is seriously affected with noise, rendering the results unreliable unless other kinds of process are taken into consideration.

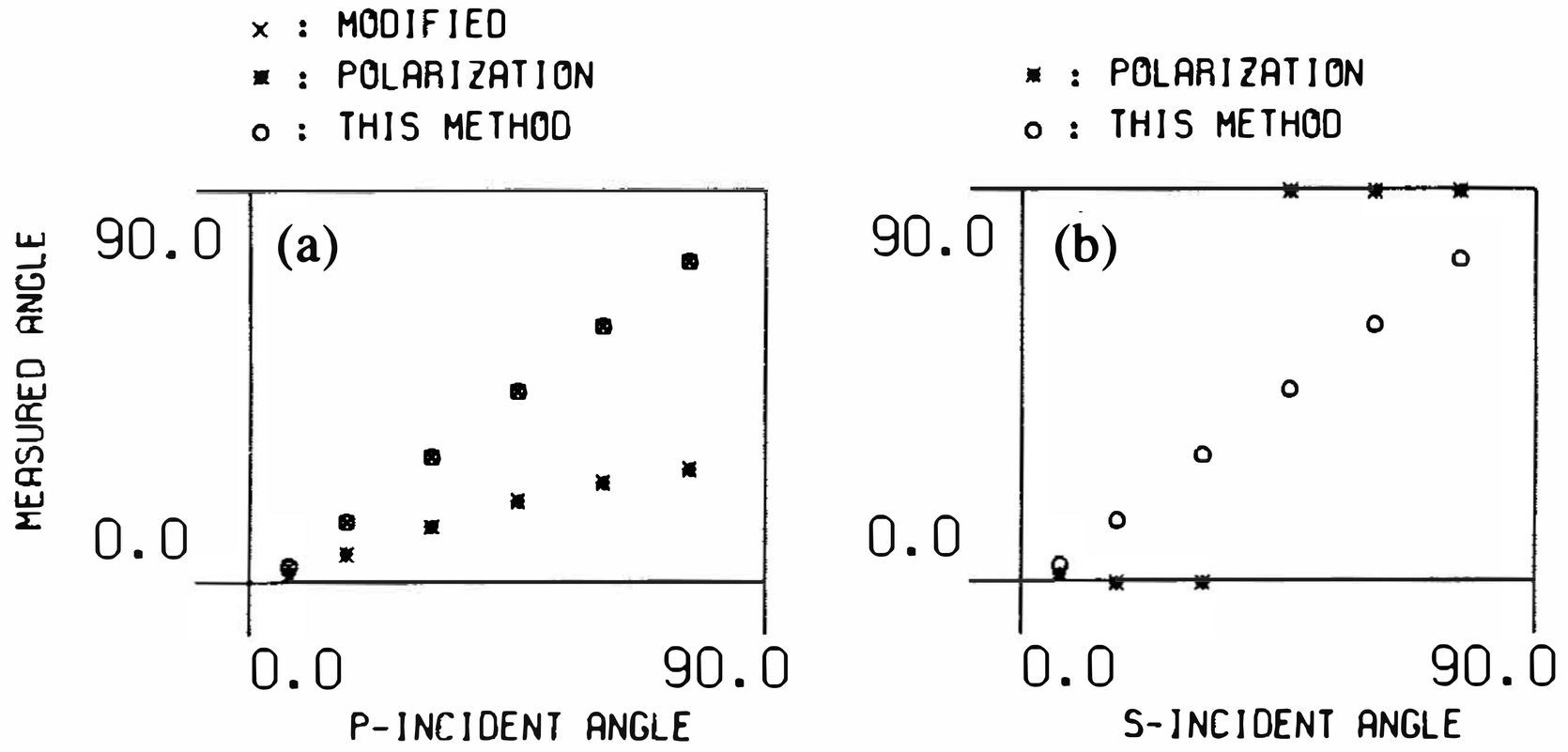

Fig. 3. The comparison of the calculated angles by the PSM and polarization method, (a) P-wave (b) SV-wave, where the asterisk "*" is the apparent angle calculated by the polarization method, " × " is the modified angle calculated by Equation (18) and " o " is the angle calculated directly by the PSM. There is no simple modified method for the SV-wave causing only the apparent angles to be displayed in (b).

3. DATA ANALYSIS

The first P- and SV-arrivals of strong motion data are extracted for the PSM analysis. To increase the S/N ratio, the extracted P- and SV-waves were bandpassed in the frequency range of 2 - 15 Hz and 1 - 5 Hz respectively. The accelerograms used in this study are from the earthquake which occured on July 30, 1986 at 1131 UT, at epicenter 121°, 47.650' E, 24°, 37.728'N at a depth 1.6 km, M_L=6.2 and which was recorded by the SMART 1 array.

Twelve accelerograms recorded by inner array (station code I01 to I12) were used, and their relative station information is listed in Table 1. The velocities of the P- and S- waves for the top 15 m of this area are 0.6 and 0.14 km/s respectively (Wen and Yeh, 1984). Before being analyzed, all of the data used in this study were rotated into the vertical, radial and transverse directions by the calculation of the azimuthal angle (Table 1) and only the vertical (Z) and the radial (R)) components were used for the PSM analysis. Figure 4 shows the first P arrival at each station, recorded in the vertical and the radial components. After the PSM analysis, the angle of incidence were obtained (marked on the top right), and the incident P wave is recovered as it was before hitting the free surface. Since the velocity of the P-wave on surface is very low, the P wave is supposed to be close to the vertical incidence, and the angle of incidence should also be very small. But the result is not as expected; one possible cause is the irregular boundary at the bottom of the Lanyang Basin (where the SMART 1 is located). From the data of Stations I02, I06, and I11, it is found that the particle motion is not linear; on the contrary, it clearly appears to be nonlinear motion. Accordingly, it is not a pure P-wave. The factors, other than background noise, to have caused this phenomenon are very complicated and are therefore not discussed here. The results of the first SV- arrival are listed in Figure 5. Comparing Figures 4 and 5, it is seen that the free surface effect has more influence on the SV-wave than on the P- wave. Figure 6 shows the angles of incidence of the P- and SV-waves, as calculated by the PSM and polarization method, and it is clear that among the data of the twelve stations, the calculated angles of the P-wave have a great variation, while those of the SV-wave show very consistent results. Since the irregular layer boundary has a greater influence on the P-wave with a higher frequency than that on the S-wave with a lower frequency, this may be attributable to the deviation of the angles of the P-waves.

When the PSM applies to the real data, only the data around the peak amplitude spectra are used. Therefore, its availability may be suspected. To test this, data from one station (I03) may be analyzed at all frequencies. Figure 7 shows the spectra of the P-wave in the

Table 1

EARTHQUAKE: July 30, 1986, 1131UT
EPICENTER: 121°, 47.650'E, 24°, 37.728'N
M_L = 6.2, DEPTH = 1.6 Km
SMART-1 INNER STATIONS

Station Code	Longitude Degree	Latitude Degree	Epicenter Distance km	Azimuth Degree
I01	121.76503.	24.67548	5.88317	329.9614
I02	121.76603	24.67503	5.88122	331.0793
I03	121.76663	24.67434	5.70828	330.8153
I04	121.76671	24.67336	5.64820	330.5714
I05	121.76620	24.67254	5.69070	330.2052
I06	121.76515	24.67206	5.71532	329.1285
I07	121.76419	24.67201	5.43725	326.1226
I08	121.76350	24.67428	5.59181	325.4115
I09	121.76277	24.67319	5.66325	325.9074
I10	121.76278	24.67410	5.76167	326.5683
I11	121.76346	24.67485	5.82538	327.8037
I12	121.76414	24.67550	5.93751	329.2470

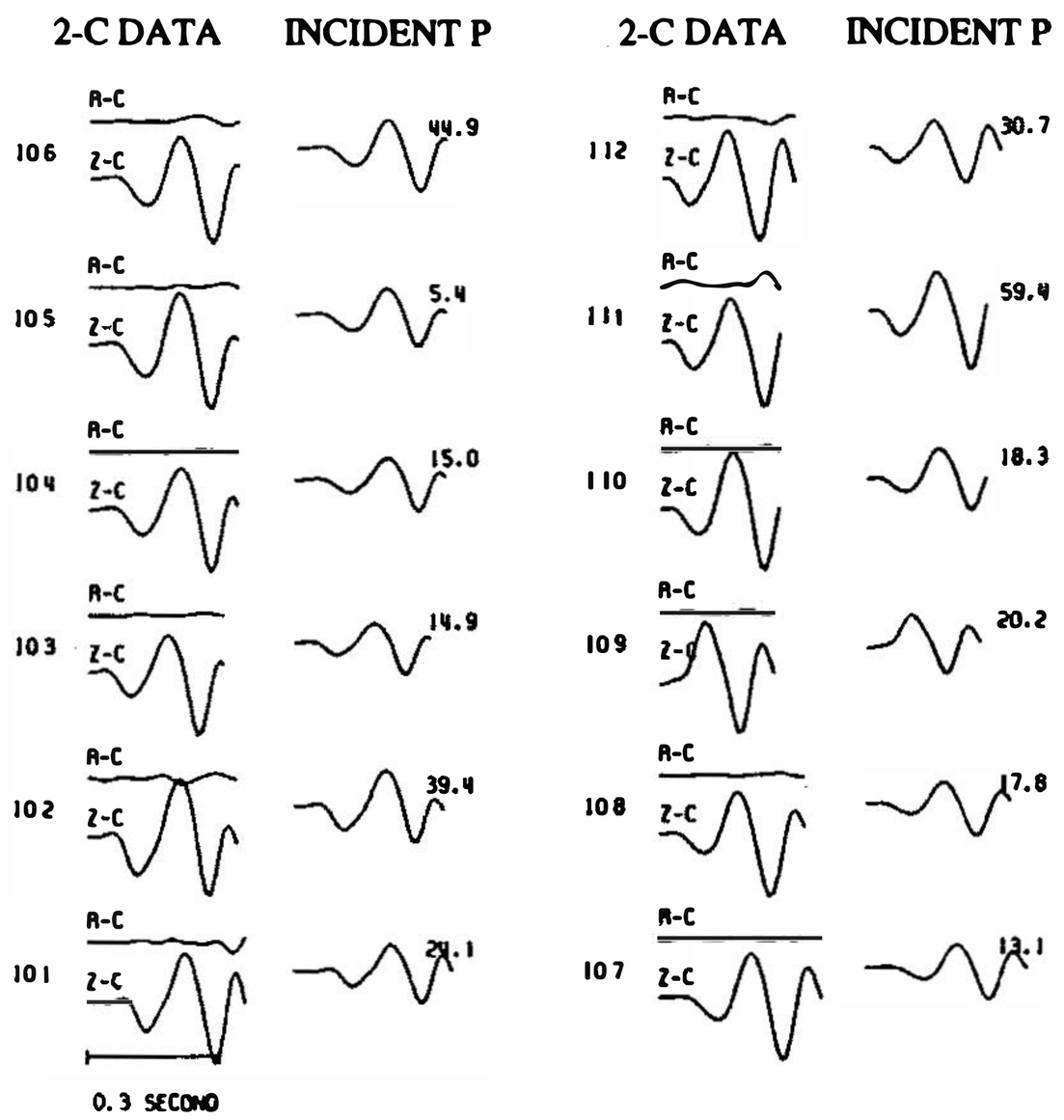

Fig. 4. The bandpass filtered (2-15 Hz) P-waves for each station are displayed on the left, and the recovered incident P-waves are shown on the right. The angles calculated by the PSM are marked on the end of the recovered signals.

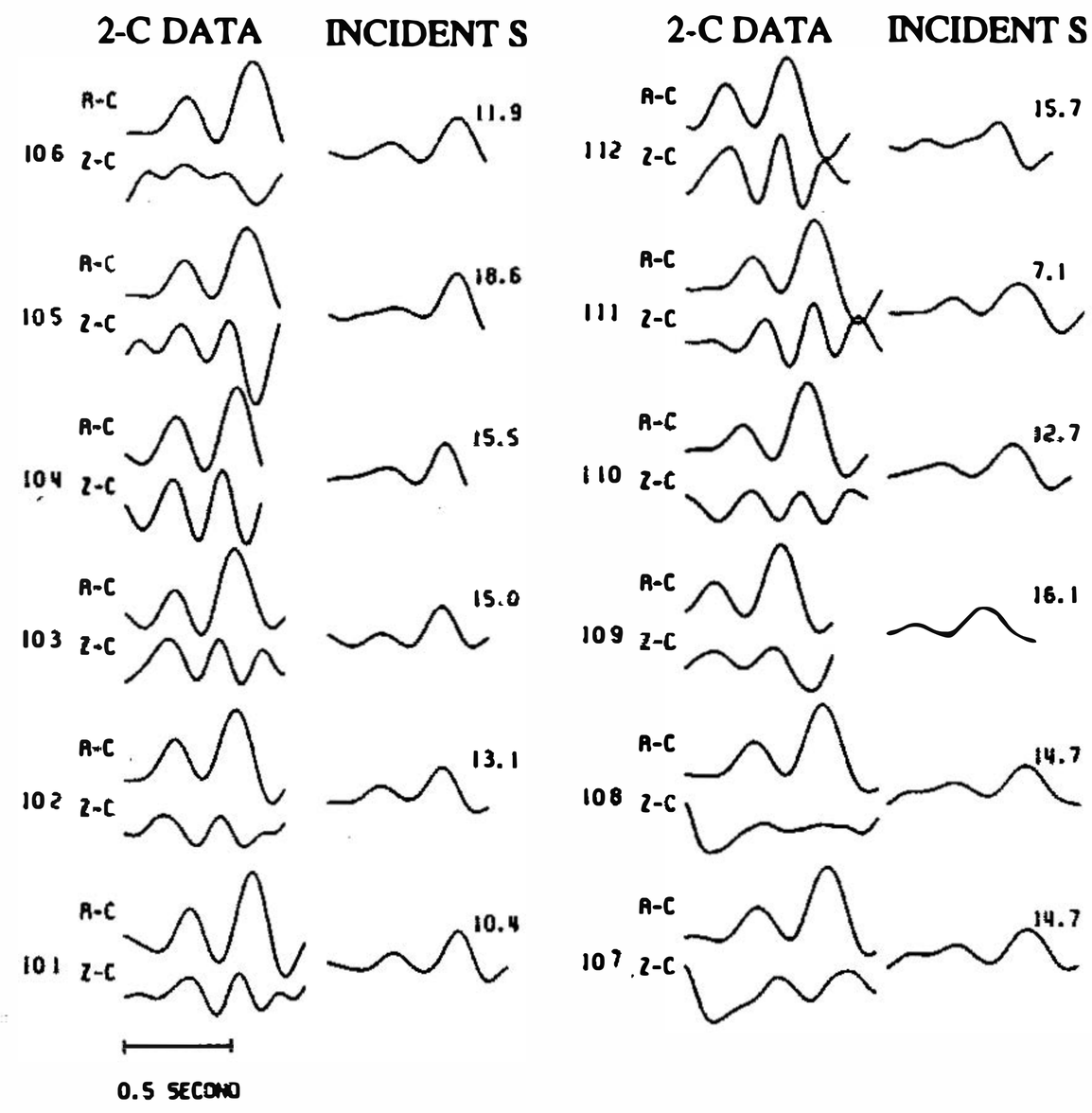

Fig. 5. The bandpass filtered (1-5 Hz) SV-waves for each station are displayed on the left, and the recovered incident SV-waves are shown on the right. The angles calculated by the PSM are marked on the end of the recovered signals.

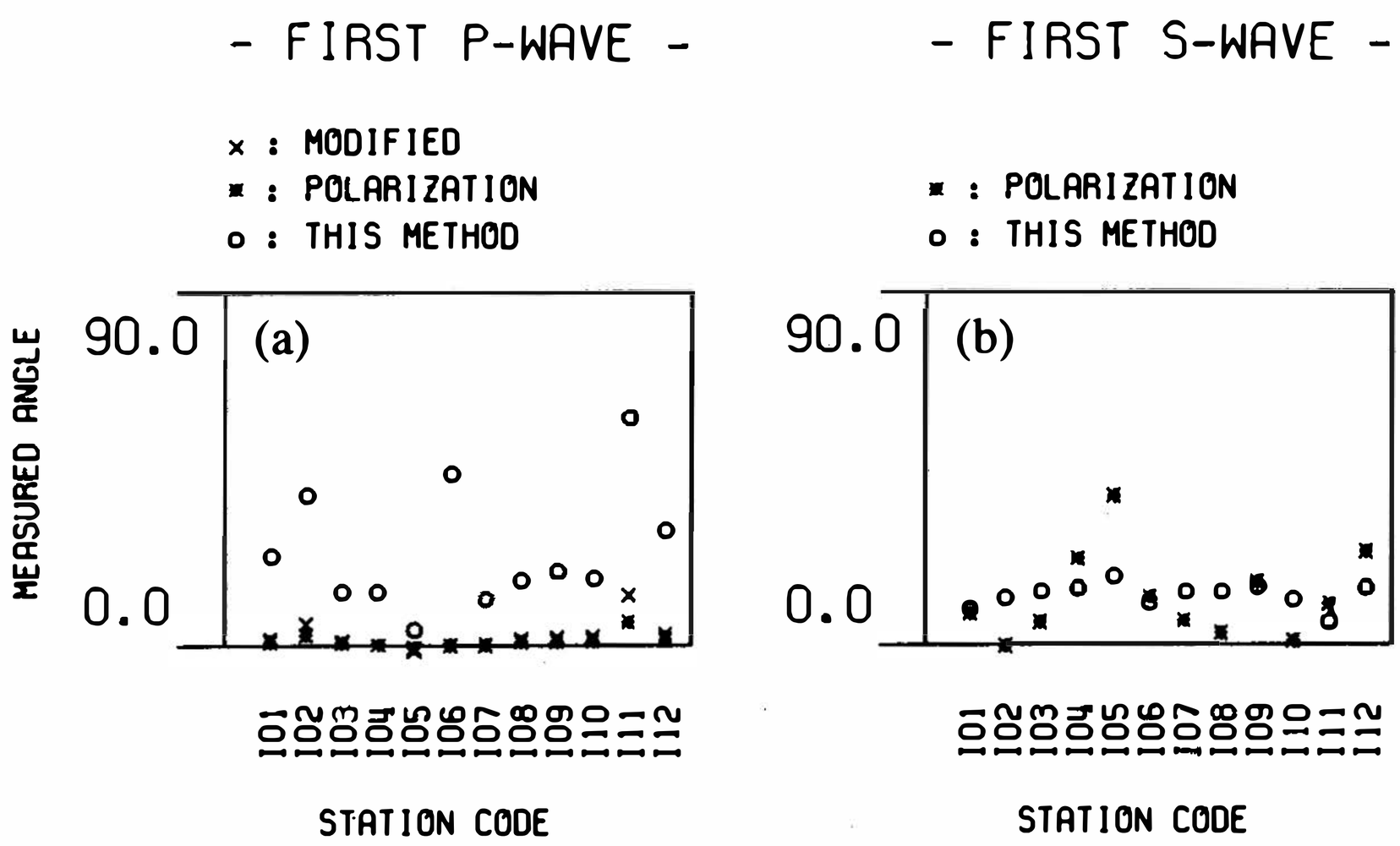

Fig. 6. The angles of incidence, (a) P- and (b) SV-waves, calculated by the PSM and polarization method without modification. The calculated angles of the P-wave have great variations, while those of the SV-wave show very consistent results.

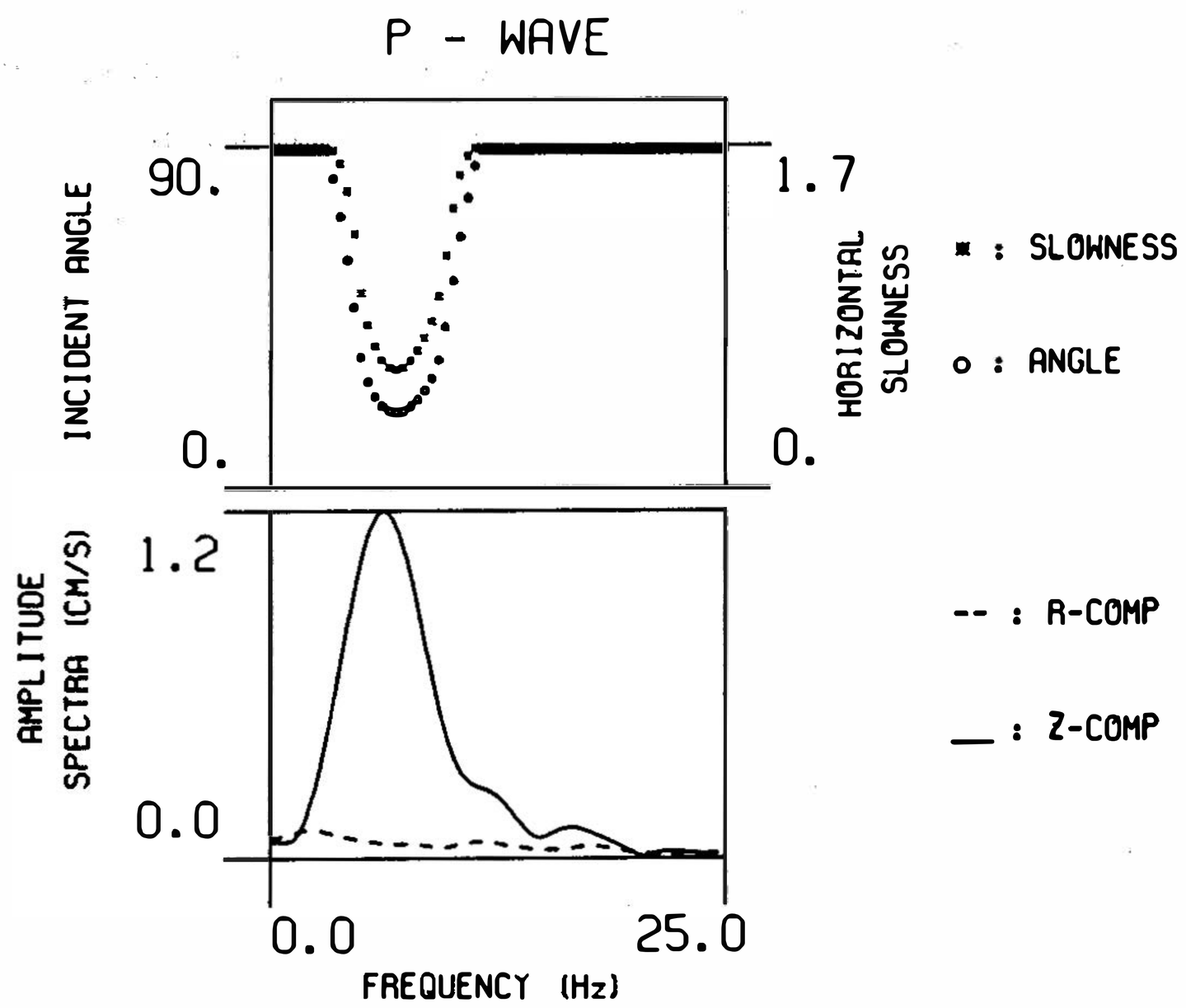

Fig. 7. The spectra of P-waves in the vertical and the radial components and the calulated angles of incidence and the slowness.

vertical and the radial components, while Figure 8 shows that of the SV-wave. Figure 7, shows that most of the P-wave energy lies in the vertical component, and its frequency range is limited in the window chosen by the PSM (2-15Hz); angles beyond this range are all 90 degrees. Likewise, most of the SV-wave energy lies in the radial component, and its frequency range is limited to the window chosen by the PSM. This demonstrates the applicability of the PSM analysis.

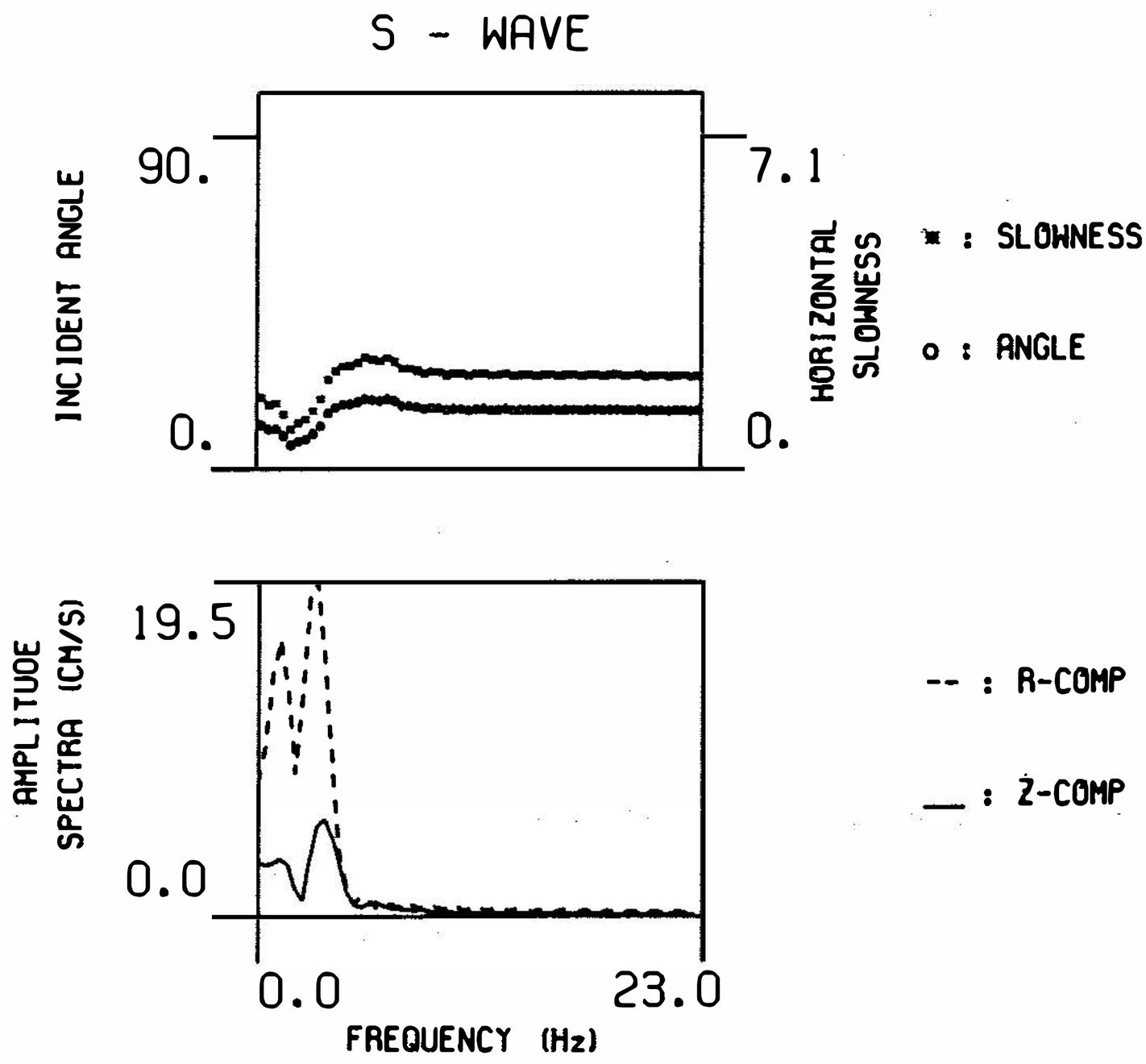

Fig. 8. **The spectra of SV-waves in the vertical and the radial components and the calculated angles of incidence and the slowness.**

4. CONCLUSIONS

The purpose of this study is to develop a simple method to find the energy ratio around the peak on amplitude spectra, and moreover, to estimate the angle of incidence and the slowness of the P- and SV-waves. The prior condition is to get an understanding of the velocity structure in the neighbourhood of the receiver. From the analysis of the synthetic results, this method proves to be correct. While being applied to practical data, it is understood that the discrepancies on the P-wave are very large, but on the SV- wave very little. The reasons may be very complicated but worthy of further investigation. From the study results, it is also found that the free surface effect has more influence on the SV-wave than on the P-wave. The PSM, when used in a single station or small array data, can estimate the ray parameter which is significant for seismic research. The waveform distortion and amplification of different incident waves can also be estimated by the PSM. In civil engineering, the knowledge of these features is of great assistance in the design and construction of buildings and infrastructure.

Acknowledgments The author appreciates the careful review of the manuscript and valuable suggestions by an anonymous reviewer. This work was supported by the National Sciences Council under contract NSC83-0202-M014-C01.

REFERENCES

Aki, K., and P. G. Richards., 1980: Quantitative seismology, W. H. Freeman, San Francisco. 932pp.

Ben-Menahem, A., and S. J. Singh., 1981: Seismic Waves and Sources, Springer-Verlag, Berlin. 1108pp.

Dankbaar, J. W. M., 1985: Separation of P- and S-waves. *Geophys. Prosp.*, **33**, 970-986.

Flinn, E. A., 1965: Signal analysis using rectilinearity and direction of particle motion. *IEEE*, **53**, 1874-1876.

Goldstein, P., and R. J. Archuleta., 1991a: Deterministic frequency-wavenumber method and direct measurements of rupture propagation during earthquakes using a dense array: theory and method. *J. Geophys. Res.*, **96**, 6173-6185.

Goldstein, P., and R. J. Archuleta., 1991b: Deterministic frequency-wavenumber method and direct measurements of rupture propagation during earthquakes using a dense array: data analysis. *J. Geophys. Res.*, **96**, 6187-6198.

Jepsen, D. C., and B. J. L. Kennett., 1990: Three component analysis of regional seismograms. *Bull. Seism. Soc. Am.*, **80**, 2032-2052.

Kennett, B. J. L., 1991: The removal of free surface interaction from three-component seismograms. *Geophys. J. Int'l.*, **104**, 153-163.

Kennett, B. J. L., 1983: Seismic Wave Propagation in Stratified Media, Cambridge University Press, Cambridge, UK. 342pp.

Wen, K.-L., and Y. T. Yeh., 1984: Seismic velocity structure beneath the SMART 1 array. *Bull. Inst. Earth Sci., Academia Sinica*, **4**, 51-72.